

# Perimeter-defense Game on Arbitrary Convex Shapes

Daigo Shishika<sup>a</sup>, Vijay Kumar<sup>a</sup>

<sup>a</sup>GRASP Lab, University of Pennsylvania, USA.

---

## Abstract

This paper studies a variant of the multi-player reach-avoid game played between intruders and defenders. The intruder team tries to score by sending as many intruders as possible to the target area, while the defender team tries to minimize this score by intercepting them. Specifically, we consider the case where the defenders are constrained to move on the perimeter of the target. Finding the optimal strategies of the game is challenging due to the high dimensionality of the joint state space. As a tractable approximation, an existing method decomposes the game into one vs. one games and reduces the design of the defense strategy to an assignment problem. To solve the one vs. one game, the existing work either relies on numerical approaches or makes simplifying assumptions (e.g., circular perimeter, or equal speed). This work provides an analytical solution to the game played on any arbitrary convex shapes. We also provide a detailed discussion on the optimality of the derived strategies. In addition, we solve the two vs. one game to introduce a cooperative defense maneuver, where a pair of defenders team up to capture an intruder that cannot be captured by either one of the defender individually. The existing assignment-based defense strategy is extended to incorporate such cooperative behaviors.

*Key words:* Pursuit evasion game, Reach avoid game, Cooperative control

---

## 1 Introduction

Maintaining perimeter surveillance and security is a complex problem given that it has become practical to deploy autonomous agents in large numbers. Various approaches to counter intrusions by unmanned vehicles have been studied including detection and tracking mechanisms [11], patrolling strategy [24], intrusion detection based on behavior rules [22], and GPS spoofing to manipulate the behavior of the agents [16].

When evasive targets need to be detected, intercepted, or surrounded, the scenarios are often formulated as pursuit-evasion games (PEGs) [7]. The game is played between two types of agents: pursuers and evaders. If it is formulated as a *game of kind*, we ask which initial configuration leads to capture (or evasion), and what pursuit (or evasive) strategy guarantees that. If it is formulated as a *game of degree*, we find the optimal strategy for a given objective function. For example, the pursuer may try to minimize the time it takes to capture, while the evader tries to maximize it.

The game becomes more complex when the evader has another objective, such as to reach a target. A version

of this problem is called the target-attacker-defender (TAD) game [27,12,19]. In a TAD game the attacker aims to capture the target while avoiding being captured by the defender, and the defender tries to defend the target by intercepting the attacker. This formulation has gained attention in missile guidance and navigation community where the attacker and the defender are both missiles [26,12]. In [19] the problem was treated with a more general agent model where the defender could save the target by reaching it before the attacker. The target can also coordinate with the defender to evade the attacker and rendezvous with the defender.

Another formulation focuses on the case where the target is some region in the game space and is no longer treated as an agent. The complexity in the attacker objective still remains the same; it has to both evade the defender and approach the target. The two-player version of the game (one defender vs. one attacker) was first introduced by Isaacs as the target-defense game [15]. This game is also called the reach-avoid game [8], and has been extended to the case with multiple players [13,6,5].

This paper considers the perimeter defense game, which is a variant of the reach-avoid game played between intruders and defenders [30]. The intruder team tries to score by sending as many intruders as possible to the target area, while the defender team tries to minimize

---

*Email addresses:* shishika@seas.upenn.edu (Daigo Shishika), kumar@seas.upenn.edu (Vijay Kumar).

this score by intercepting them. A specific assumption made in this paper is that the defenders are constrained to move on the perimeter. Such assumption is motivated by the scenarios where the target region acts as an obstacle that the defenders cannot move through ( e.g., defending a perimeter of a building using ground vehicles).

Various solution methods have been proposed to solve the PEGs introduced thus far. In general the approaches can be divided into two types: the differential game formulation and the explicit policy method [19]. The former obtains the strategies and the winning regions by solving a Hamilton-Jacobi-Isaacs (HJI) partial differential equation (PDE), while the latter analyzes the outcome of the game by prescribing a strategy to the players.

The differential game formulation has been successfully utilized for relatively simple problems that allow analytical solution to the HJI PDEs [15,3,20], and other problems with low dimensional state space for which the HJI PDEs can be numerically solved [9,6]. The strength of this approach is that the optimality of the derived strategies are ensured by construction. The down side is the curse of dimensionality, which makes the HJI PDEs intractable for problems with large state space. This is why the explicit policy method is widely used for multi-player PEGs.

For scenarios involving multiple pursuers, specific control strategies have been proposed with the analyses on their performance guarantees. Approaches based on Voronoi tessellation and area minimization can be found in various works [14,32,25]. A variant of such work proposes a so called relay pursuit to improve the overall efficiency by selecting one pursuer to actively go after the evader [2], and it has been applied to a more complex scenario [29]. A behavior called the cyclic pursuit uses a chain of pursuers to encircle a target [17,4]. For a non-adversarial scenario where there is no evasive maneuver, the problem is formulated as the vehicle-routing problem [31,1]. Evasive maneuvers have also been considered in the scenario with one pursuer and multiple evaders [10,28].

The problem becomes more challenging when there are multiple pursuers and multiple evaders. The underlying question is “which pursuer should go after which evader?” In [25], a Voronoi-tessellation based approach was used to directly obtain the desired direction of motion. In [21], a task allocation approach was proposed, where the solution to the multiple pursuers vs. one evader problem was used to assign a unique pursuer for each evader so that capture in minimum time is guaranteed. When there were multiple evaders assigned to a single pursuer, Voronoi tessellation was used to select a single evader that is closest [21].

Specifically for the reach-avoid game played between multiple defenders and multiple attackers, [6] approxi-

mated the multi-player game as a combination of two-player games. In contrast to a more conventional PEG that considers the time of capture, we need to consider whether the given pursuer can capture the attacker before it reaches the target. To obtain this feasibility (capturability) information, the solutions to the two player games (strategies and winning regions) were obtained by numerically solving the associated HJI PDE [6]. These solutions were used to formulate the design of defense policy as an assignment problem.

Following the approach taken in [6], this paper starts by identifying the solution to the two player game: the game played between one defender and one intruder. Although the two-player game has been solved either numerically [6,5], or under restricted assumptions (circular perimeter or equal speed) [30], we analytically solve the problem for arbitrary convex shapes. This is enabled due to the constraint that the defender moves on the perimeter.

In addition, the derived solution exhibits an interesting contrast to the solution obtained using the concept called the dominance region, which was used in the original work by Isaacs [15] and also in [23]. The intruder-dominated region contains all the points in the game space that the intruder can reach first regardless of the defender’s strategy [23]. One can conclude that the intruder reaches the target/perimeter if the intruder-dominated region intersects with the target region. However, our analysis shows that such condition is only sufficient and not necessary. This is another consequence of the unique assumption that the target region also behaves as an obstacle.

We also extend the existing assignment method by incorporating a cooperative defense performed by two defenders. To this end, we analytically solve the game played between two defenders and one intruder. Then the solution to this two vs. one game is incorporated in the extended assignment policy.

The contributions of the paper are (i) the solution to the one v.s. one (1v1) game; (ii) the solution to the two v.s. one (2v1) game that shows the benefit of defender cooperation; (iii) the analysis on the optimality of the derived strategies; and (iv) the assignment policy that accommodates the defender cooperation.

In the previous work [30] the perimeter-defense game was solved on a circular perimeter with a formulation that is not applicable to general shapes. This paper uses a formulation that can treat any convex shapes including the circular perimeter. The extension to polygonal perimeter was discussed in [30], but the result was limited to the case where the defender and the intruder had the same speed limits. This paper accommodates a more general case where the defender has any speed that is equal or higher than the intruder. Finally, the discussion

of the payoff functions that makes the derived strategies optimal has not been published before.

Section 2 formulates the problem. Section 3 solves the game played by one defender and one intruder (1v1 game). Section 4 introduces the cooperative aspect by solving the game played by two defender and one intruder (2v1 game). Section 5 proposes the defender team strategy using the results of 1v1 and 2v1 games. Section 6 presents the numerical results. Section 7 concludes the paper.

## 2 Problem formulation

This section formulates the reach-avoid game for defenders constrained on a perimeter. The target  $\mathcal{T} \subset \mathbb{R}^2$  is assumed to be a convex region on a plane, and its perimeter is given by an arc-length parameterized curve  $\gamma : [0, L) \rightarrow \partial\mathcal{T}$ , where  $L$  denotes the perimeter length. We use  $s \in [0, L)$  to denote the arc-length position on the curve. The tangent vector of the curve at  $s$  is denoted by  $\mathbf{T}(s) \triangleq \frac{d\gamma(s)}{ds}$ .

For any two points/vectors in  $\mathbb{R}^2$  we denote the relative vectors using

$$\mathbf{x}_{a \rightarrow b} \triangleq \mathbf{x}_b - \mathbf{x}_a,$$

and the unit vectors using  $\hat{\mathbf{x}} = \frac{\mathbf{x}}{\|\mathbf{x}\|}$ . The arc-length from point  $s_a$  to  $s_b$  on the curve in counter-clockwise (ccw) direction is denoted by

$$s_{a \rightarrow b} \triangleq (s_b - s_a) \bmod L,$$

for example,  $s_{a \rightarrow b} + s_{b \rightarrow a} = L$ . The segment starting from  $s_a$  and ending at  $s_b$  in ccw direction is denoted by  $[s_a, s_b] \triangleq \{s_x \mid s_{a \rightarrow x} \leq s_{a \rightarrow b}\}$ . We use  $(s_a, s_b)$  when the endpoints are not included.

A set of  $N_D$  defenders  $\{D_i\}_{i=1}^{N_D}$  are constrained to move on the perimeter. This assumption is motivated by defending the perimeter of a building that the agents cannot move through. The position of the  $i$ th defender is described by  $s_{D_i}$  or  $\mathbf{x}_{D_i} = \gamma(s_{D_i})$ . The defender's control input is the signed speed;  $\dot{s}_{D_i} = \omega_{D_i}$  or  $\dot{\mathbf{x}}_{D_i} = \omega_{D_i} \mathbf{T}(s_{D_i})$  with the constraint  $|\omega_{D_i}| \leq 1$ .

A set of  $N_A$  intruders  $\{A_j\}_{j=1}^{N_A}$  have first-order integrator dynamics in  $\mathbb{R}^2$ . The control inputs are the velocities;  $\dot{\mathbf{x}}_{A_j} = \mathbf{u}_{A_j}$  with the constraint  $\|\mathbf{u}_{A_j}\| \leq \nu$ . It is assumed that the defender is faster:

$$\nu \in (0, 1]. \quad (1)$$

We assume that each player has the perfect state information and the speed ratio  $\nu$  is also known.

In a microscopic view, an intruder  $A_i$  scores if it reaches the target ( $\mathbf{x}_{A_i} \in \partial\mathcal{T}$ ) without being captured by the

defenders. We use zero distance to define capture. The defender moves on the perimeter to either intercept the intruder or prevent it from scoring indefinitely.

As the building blocks to analyze the multi-player game, we solve the game played by one defender and one intruder, and also by two defenders and one intruder.

**Problem 1:** Find the surface that divides the state space into intruder-winning and defender-winning configurations. In each region, what are the optimal strategies to be adopted by the players?

In a macroscopic view, we use  $Q \in \mathbb{N}$  to denote the number of intruders that reach the perimeter. The intruder team maximizes  $Q$  while the defender team minimizes it.

**Problem 2:** Given an initial configuration of the game and the speed ratio  $\nu$ , what is the upper bound on the score  $Q$  and the defender strategy to ensure that bound?

We address these problems in the following sections.

## 3 Two Player Game

This section solves the game played between one defender and one intruder. The states of the system are  $[s_D, \mathbf{x}_A]$  and the dynamics are  $[\dot{s}_D, \dot{\mathbf{x}}_A] = [\omega_D, \mathbf{u}_A]$ . The terminal condition corresponding to intruder's win is  $\mathbf{x}_A \in \mathcal{T}$ . The terminal condition for defender's win is discussed later in Sec. 3.2.

We first introduce the relevant geometries, and then solve the game of kind to find the surface called the *barrier* that divides the game space into the intruder-winning configuration and the defender-winning configuration. We also discuss the objective functions for which the derived strategies are also optimal in the game of degree.

### 3.1 Geometries

Let  $s_{\text{tan,R}}$  and  $s_{\text{tan,L}}$  denote the points where the tangent lines from  $\mathbf{x}_A$  touches the perimeter (see Fig. 1a). Considering the directions from the perspective of a defender facing outward from the perimeter, the subscript  $\text{R}$  corresponds to the "right" or clockwise (cw) direction of motion, and  $\text{L}$  corresponds to the "left" or counter-clockwise (ccw). We use

$$\mathcal{S}_d(\mathbf{x}_A) \triangleq [s_{\text{tan,R}}, s_{\text{tan,L}}]$$

to denote all the points on the perimeter that the intruder can reach on a straight line. Note that these geometries are independent of the defender position.

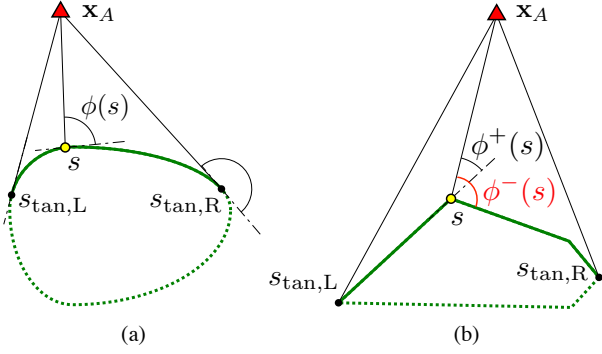


Fig. 1. Illustration of the tangent points and the approach angle. The segment  $\mathcal{S}_d$  is indicated with the solid line. (a) For a smooth perimeter. (b) For a polygonal perimeter.

For a given point  $s_B \in \mathcal{S}_d$ , consider the following quantity:

$$J_L(s_B; s_D, \mathbf{x}_A) \triangleq s_{D \rightarrow B} - \frac{\|\gamma(s_B) - \mathbf{x}_A\|}{\nu}. \quad (2)$$

The first term is the ccw distance from the defender to  $s_B$ , and  $\|\gamma(s_B) - \mathbf{x}_A\|$  is the distance from the intruder to  $s_B$ . Hence, recalling that the defender and the intruder has the speed 1 and  $\nu$  respectively,  $J_L$  describes how much longer it takes for the defender to reach  $s_B$  than the intruder, when the defender moves ccw and the intruder moves on a straight line path towards  $s_B$ . The subscript  $L$  is used to highlight that we assume the engagement in the “left” or ccw direction.

Suppose the game starts at  $t = 0$  and the intruder reaches  $s_B$  at time  $t_F$  before the defender does. Then  $s_{D \rightarrow B}(t_F) = s_{D \rightarrow B}(0) - t_F \omega_D \geq s_{D \rightarrow B}(0) - t_F = s_{D \rightarrow B}(0) - \frac{\|\gamma(s_B) - \mathbf{x}_A\|}{\nu}$ . Therefore, a positive  $J_L(s_B)$  can also be interpreted as the arc-length distance between the intruder and the defender when the intruder reaches  $s_B$ . To focus on the geometry, we defer the question of defender’s optimal direction of motion, and whether the intruder should employ straight line path, to the later sections.

Restricting ourselves to straight line paths for now, the intruder maximizes  $J_L$  by finding the optimal breaching point  $s_B$ . The derivative is given by

$$\begin{aligned} \frac{dJ_L}{ds_B} &= \frac{d}{ds_B}(s_B - s_D) - \frac{1}{\nu} \frac{d}{d\gamma} \|\gamma - \mathbf{x}_A\| \cdot \frac{d\gamma(s_B)}{ds_B} \\ &= 1 - \frac{1}{\nu} \frac{\gamma(s_B) - \mathbf{x}_A}{\|\gamma(s_B) - \mathbf{x}_A\|} \cdot \mathbf{T}(s_B), \end{aligned}$$

where the dot product in the second term is related to the *approach angle* defined in the following:

**Definition 1** Suppose the intruder position  $\mathbf{x}_A$  is given. Then for  $s \in \mathcal{S}_d$ , we define the **approach angle** to be

$$\phi(s) \triangleq \cos^{-1} \left( \frac{\gamma(s) - \mathbf{x}_A}{\|\gamma(s) - \mathbf{x}_A\|} \cdot \mathbf{T}(s) \right) \in (0, \pi). \quad (3)$$

For a perimeter with discontinuous tangent vector (e.g., polygonal perimeter), we use  $\phi^-(s)$  and  $\phi^+(s)$  to denote the approach angle before and after the discontinuity (in ccw direction).

Note that  $\phi$  is non-increasing from right to left due to the convexity of  $\mathcal{T}$ , and for a smooth perimeter, we always have  $\phi(s_{\text{tan,R}}) = \pi$  and  $\phi(s_{\text{tan,L}}) = 0$  (see Fig. 1b).

Using the approach angle, the partial derivative is described as:

$$\frac{dJ_L}{ds_B} = 1 - \frac{\cos \phi(s_B)}{\nu},$$

which gives the following:

$$\frac{dJ_L}{ds_B} = \begin{cases} \text{positive} & \text{if } \phi(s_B) > \phi_L^* \\ 0 & \text{if } \phi(s_B) = \phi_L^* \\ \text{negative} & \text{otherwise.} \end{cases} \quad (4)$$

where

$$\phi_L^* = \cos^{-1}(\nu).$$

This result provides the critical breaching point that maximizes  $J_L$  as follows:

**Definition 2** We define **left breaching point**  $s_L(\mathbf{x}_A) \in \mathcal{S}_d$  to be the point that maximizes  $J_L^*$ . For a differentiable  $\gamma(s)$ , it is the unique solution of  $\phi(s) = \phi_L^*$ , i.e.,

$$s_L(\mathbf{x}_A) = \phi^{-1}(\cos^{-1} \nu). \quad (5)$$

For a non-smooth perimeter,  $s_L(\mathbf{x}_A)$  is a unique point that satisfies either of the following conditions:

$$\begin{cases} \phi(s) = \phi_L^* & (s_L \text{ is on an edge}), \\ \phi(s)^+ < \phi_L^* < \phi(s)^- & (s_L \text{ is on a vertex}). \end{cases} \quad (6)$$

Due to the monotonicity of  $\phi(s)$  on a convex perimeter,  $s_L$  is always unique, and it can be found by a simple search on a one-dimensional space. It is also obtained analytically for some special cases (see Sec. 3.4)

**Remark 1 (Limiting cases)** When  $\nu = 1$ , then we always have  $s_L = s_{\text{tan,L}}$ , because  $\phi_L^* = 0$ . When  $\nu \rightarrow 0$  the optimal approach angle is  $\phi_L^* \rightarrow \frac{\pi}{2}$ . Therefore,  $s_L$  is equivalent to the closest point on the perimeter from  $\mathbf{x}_A$ .

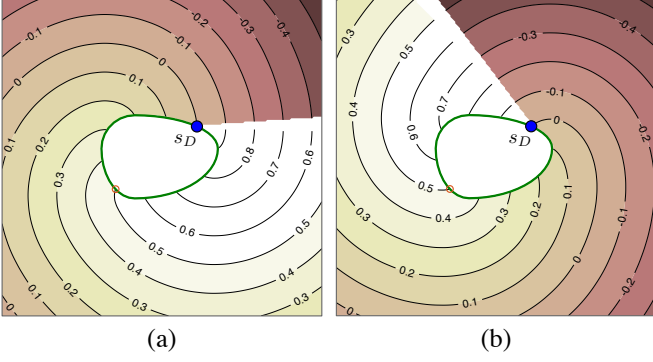


Fig. 2. Level sets of  $J_L^*(s_D, \mathbf{x}_A)$  (left) and  $J_R^*(s_D, \mathbf{x}_A)$  (right) for a fixed value of  $s_D$ .

Noting the dependencies on  $s_D$  and  $\mathbf{x}_A$ , we define a function for the critical value of  $J_L$  as follows:

$$J_L^*(s_D, \mathbf{x}_A) \triangleq J_L(s_L) = \max_{s_B \in \mathcal{S}_d} J_L(s_B). \quad (7)$$

For a similar analysis on the cw motion of the defender, consider the following function:

$$J_R(s_B; s_D, \mathbf{x}_A) = s_{B \rightarrow D} - \frac{\|\mathbf{x}_A - \gamma(s_B)\|}{\nu}. \quad (8)$$

The arc-length computation changed from  $s_{D \rightarrow B}$  to  $s_{B \rightarrow D}$ . With the same process, we can show that  $J_R$  is maximized by the *right breaching point* defined as the solution to

$$\phi(s_R) = \phi_R^* = \pi - \cos^{-1}(\nu). \quad (9)$$

We define a function for the critical value as

$$J_R^*(s_D, \mathbf{x}_A) \triangleq J_R(s_R) = \max_{s_B \in \mathcal{S}_d} J_R(s_B). \quad (10)$$

Figure 2 shows the level sets of  $J_L^*$  and  $J_R^*$  for a fixed value of  $s_D$ . There is a discontinuity along the manifold where  $s_L(\mathbf{x}_A) = s_D$ .

Next we use the two functions  $J_L^*$  and  $J_R^*$  to divide the game space into “right side” and “left side” based on the position of the defender. Let  $s_D^{\text{op}}$  be the farthest (opposite) point from the defender on the perimeter. The partitioning will be given by the surface defined in the following:

**Definition 3** Consider the surfaces defined by

$$\Gamma(s_D) = \{\mathbf{x}_A \mid J_L^*(\mathbf{x}_A, s_D) = J_R^*(\mathbf{x}_A, s_D)\}. \quad (11)$$

The one extending from  $s_D$  is called the **afferent surface**,  $\Gamma_{\text{aff}}$ , and the other extending from  $s_D^{\text{op}}$  is called the **dispersal surface**,  $\Gamma_{\text{dis}}$  (see Fig. 3a).

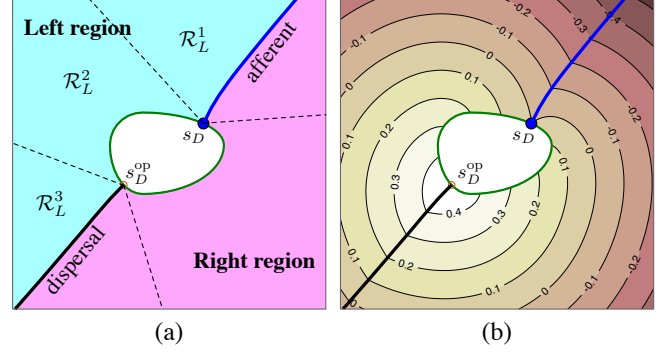


Fig. 3. Singular surfaces. (a) Left region (cyan) and right region (magenta). The left region is further partitioned into three regions. (b) Level sets of  $V$ .

The singular surfaces are defined in the three-dimensional state space, but for convenience, we look at the “two-dimensional slice” by considering specific value of  $s_D$ . The singular surfaces divide the entire game space into two regions. We define them as **left region**,  $\Omega_L(s_D)$ , and the **right region**,  $\Omega_R(s_D)$  (see Fig. 3a).

Let  $\mathcal{S}_L = [s_D, s_D^{\text{op}}]$  and  $\mathcal{S}_R = [s_D^{\text{op}}, s_D]$  denote the segments of the perimeter to the left and right of the defender. Whether the intruder is in the left region or not can be tested using the location of the breaching points ( $s_L$  and  $s_R$ ), and the relation between the values  $J_L^*$  and  $J_R^*$ . If  $\mathbf{x}_A \in \Omega_L(s_D)$ , then  $\mathbf{x}_A$  is in one of the following three regions (see Fig. 3a):

$$\begin{aligned} \mathcal{R}_L^1 &= \{\mathbf{x}_A \mid s_L \in \mathcal{S}_L, s_R \in \mathcal{S}_R, J_L^* > J_R^*\} \\ \mathcal{R}_L^2 &= \{\mathbf{x}_A \mid s_L \in \mathcal{S}_L, s_R \notin \mathcal{S}_R\} \\ \mathcal{R}_L^3 &= \{\mathbf{x}_A \mid s_L \notin \mathcal{S}_L, s_R \notin \mathcal{S}_R, J_L^* < J_R^*\}. \end{aligned} \quad (12)$$

If the states  $(s_D, \mathbf{x}_A)$  satisfy none of the above three conditions, then we know that  $\mathbf{x}_A \in \Omega_R(s_D)$ .

Finally, we merge the two objective functions as follows:

$$V(\mathbf{x}_A, s_D) = \begin{cases} J_L^*(\mathbf{x}_A, s_D) & \text{if } \mathbf{x}_A \in \Omega_L(s_D) \\ J_R^*(\mathbf{x}_A, s_D) & \text{otherwise.} \end{cases} \quad (13)$$

Fig. 3b shows the level sets of  $V(s_D, \mathbf{x}_A)$ . We later show in Sec. 3.3 that this is the *value of the game* (of degree) for some payoff functions.

### 3.2 Winning Regions

This section proves that the barrier (for the game of kind) is given by the level set  $V = 0$ . We take the explicit policy method [19] in which the game is analyzed with a specific strategy given to the player.

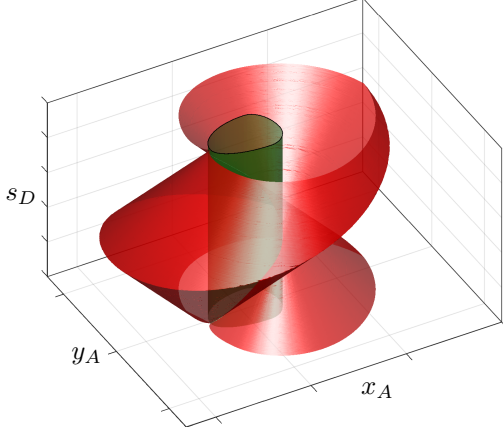


Fig. 4. Intruder winning region. The barrier surface is depicted in red. The green cylinder depicts the perimeter shape extruded vertically.

Fig. 4 depicts the surface  $V(s_D, \mathbf{x}_A) = 0$  in the three dimensional state space. For convenience, we perform our analysis using the two-dimensional slice at  $s_D$  corresponding to the location of the defender. We define the intruder winning region by

$$\mathcal{R}_A(s_D) = \{\mathbf{x}_A \mid V(s_D, \mathbf{x}_A) > 0\}. \quad (14)$$

We first show that the intruder can guarantee its victory if it starts in  $\mathcal{R}_A$ .

**Lemma 1** *If the initial configuration is such that  $\mathbf{x}_A \in \mathcal{R}_A(s_D)$  (i.e.,  $V > 0$ ), then regardless of the defender strategy, the intruder wins by the following strategy:*

$$\mathbf{u}_A^* = \begin{cases} \nu \hat{\mathbf{x}}_{A \rightarrow L} & \text{if } \mathbf{x}_A \in \Omega_L(s_D) \\ \nu \hat{\mathbf{x}}_{A \rightarrow R} & \text{otherwise,} \end{cases} \quad (15)$$

where  $\hat{\mathbf{x}}_{A \rightarrow L} = \gamma(s_L) - \mathbf{x}_A$ .

**PROOF.** Suppose  $\mathbf{x}_A \in \Omega_L(s_D)$  without the loss of generality. We consider two cases: (i)  $s_L \in [s_D, s_D^{\text{op}}]$ , and (ii)  $s_L \in [s_D^{\text{op}}, s_D]$ . In either case, we know that the intruder reaches  $s_L$  first if the defender moves ccw, because  $J_L^* = V > 0$ .

In the first case when  $s_L \in [s_D, s_D^{\text{op}}]$ , it is clear that the cw motion by the defender takes longer time to reach  $s_L$  than the ccw motion since  $s_{L \rightarrow D} > s_{D \rightarrow L}$ . Therefore, the intruder can move towards  $s_L$  and reach it no matter what the defender does. All the intruder positions corresponding to the first case are shown as the shaded region in Fig. 5.

The second case is more subtle since by moving cw, the defender may be able to reach  $s_L$  before the intruder does. Suppose the defender takes this strategy:  $\omega_D = -1$

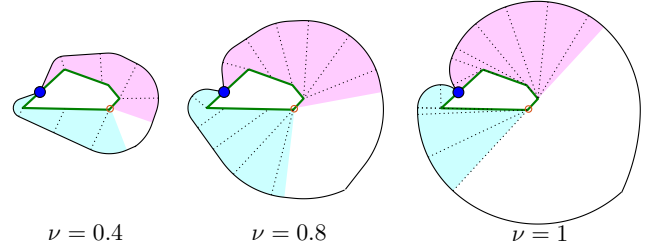


Fig. 5. Intruder-winning region under the constraint  $s_L \in \mathcal{S}_L$  (cyan) and  $s_R \in \mathcal{S}_R$  (magenta), for varied intruder speed  $\nu$ . The dotted lines illustrate the corresponding intruder paths.

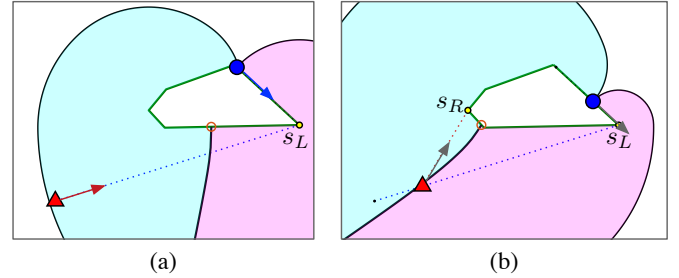


Fig. 6. Engagement when the game starts in a configuration with  $s_L \notin \mathcal{S}_L$  and  $s_R \notin \mathcal{S}_R$ . (a) Defender takes a suboptimal strategy aiming at  $s_L$ . (b) Intruder enters the right region  $\Omega_R$  and switches its motion to  $s_R$ .

(cw motion). Then  $J_L^*$  starts increasing because  $s_{D \rightarrow L}$  in (7) increases. Now, there exists a time  $t_1$  when  $\mathbf{x}_A(t_1) \in \Gamma_{\text{dis}}(s_D(t_1))$ , at which point we have

$$V(t_1) = J_L^*(t_1) = J_R^*(t_1) > J_L^*(t_0) = V(t_0) > 0. \quad (16)$$

If the defender continues in cw direction, then the intruder enters the right region ( $\mathbf{x}_A \in \Omega_R$ ), and the strategy (15) switches the breaching point to  $s_R$ . The intruder will reach  $s_R$  first because  $J_R^*(t_1) > 0$ . If the defender goes back to ccw motion, then the intruder stays in  $\Omega_L$ , and it will continue towards  $s_L$ . The intruder will reach  $s_L$  first because  $J_L^*(t_1) > 0$ . Therefore, no matter what decision the defender makes at this point,  $V(s_D, \mathbf{x}_A)$  stays positive through out the game, and the intruder never leaves  $\mathcal{R}_A(s_D)$  until it reaches the perimeter. Note if the defender continues to switch between cw and ccw motion, then the intruder will approach  $s_D^{\text{op}}$  moving along  $\Gamma_{\text{dis}}$ , and there will be no “dead-lock” situation. ■

**Remark 2 (Dominance region)** *Notice that for the configuration in Fig. 6a, the analysis based on the dominance region [23] will not conclude that the intruder can win the game, because  $s_L$  is not in the intruder-dominated region; i.e., the defender has a way to reach  $s_L$  before the intruder. Nevertheless, we have shown that the intruder can win the game by employing a closed-loop (feedback) strategy (15). Such discrepancy arises because of the fol-*

lowing two points: (i) the perimeter acts as an obstacle, and (ii) the defender is protecting a region (and not a single point).

The above Lemma 1 only gives a sufficient condition for the intruder to win. To show that it is also a necessary condition, we study what happens if the game starts in the configuration  $\mathbf{x}_A \notin \mathcal{R}_A(s_D)$ .

The defender wins the game by either intercepting the intruder or preventing it from reaching the perimeter indefinitely. For the latter scenario, we show that the defender is able to stabilize the system around the configuration  $\mathbf{x}_A \in \Gamma_{\text{aff}}(s_D)$ .

**Lemma 2** *When  $\mathbf{x}_A(t_0) \in \Gamma_{\text{aff}}(s_D(t_0))$ , then regardless of the intruder's control, the defender can maintain the condition  $\mathbf{x}_A(t) \in \Gamma_{\text{aff}}(s_D(t))$  for all  $t > t_0$  by the following control:*

$$\omega_D^*(s_D, \mathbf{x}_A) = \begin{cases} 1 & \text{if } \mathbf{x}_A \in \Omega_L(s_D) \\ -1 & \text{otherwise.} \end{cases} \quad (17)$$

**PROOF.** In the neighborhood of the surface  $\Gamma_{\text{aff}}(s_D)$ , consider the error function  $e = J_L^* - J_R^*$ . Noting that  $e > 0$  if  $\mathbf{x}_A \in \Omega_L(s_D)$  and  $e < 0$  otherwise, we can rewrite the control as  $\omega_D^* = \text{sgn}(e)$ . (Note, this expression of control is only valid in the neighborhood of  $\mathbf{x}_A \in \Gamma_{\text{aff}}(s_D)$ .) The time derivative of the squared error is  $\frac{d}{dt}e^2 = 2e(\dot{J}_L^* - \dot{J}_R^*)$ , where  $\dot{J}_L^*$  is

$$\begin{aligned} \frac{dJ_L^*}{dt} &= \dot{s}_L - \dot{s}_D - \frac{\hat{\mathbf{x}}_{A \rightarrow L}}{\nu} \cdot (\dot{s}_L \mathbf{T}(s_L) - \mathbf{u}_A) \\ &= \dot{s}_L \left( 1 - \frac{\cos \phi(s_L)}{\nu} \right) + \frac{\hat{\mathbf{x}}_{A \rightarrow L}}{\nu} \cdot \mathbf{u}_A - \omega_D \\ &= \frac{\hat{\mathbf{x}}_{A \rightarrow L}}{\nu} \cdot \mathbf{u}_A - \omega_D. \end{aligned} \quad (18)$$

From the second to the third line, we used the fact that  $\dot{s}_L \left( 1 - \frac{\cos \phi(s_L)}{\nu} \right) = 0$ , which we prove in the following. Observe that a small displacement in  $\mathbf{x}_A$  moves  $s_L$  if it is on a smooth part of the perimeter, but  $s_L$  will remain stationary if it is on a vertex (see (6)). When  $s_L$  is on a smooth part, we have  $\phi(s_L) = \phi_L^* = \cos^{-1} \nu$ , which gives  $1 - \frac{\cos \phi(s_L)}{\nu} = 0$ . When  $s_L$  is on a vertex and not moving, we have  $\dot{s}_L = 0$ .

With a similar computation on  $\dot{J}_R^*$ , the time derivative of the squared error is

$$\begin{aligned} \frac{\nu}{2} \frac{d}{dt}e^2 &= e(\hat{\mathbf{x}}_{A \rightarrow L} \cdot \mathbf{u}_A - \nu \omega_D^* - (\hat{\mathbf{x}}_{A \rightarrow R} \cdot \mathbf{u}_A + \nu \omega_D^*)) \\ &= e((\hat{\mathbf{x}}_{A \rightarrow L} - \hat{\mathbf{x}}_{A \rightarrow R}) \cdot \mathbf{u}_A - 2\nu \omega_D^*) \end{aligned}$$

Recalling that  $\hat{\mathbf{x}}_{A \rightarrow L}$  and  $\hat{\mathbf{x}}_{A \rightarrow R}$  are unit vectors, notice that  $\|\hat{\mathbf{x}}_{A \rightarrow L} - \hat{\mathbf{x}}_{A \rightarrow R}\| \leq 2$ , and the equality holds when  $\hat{\mathbf{x}}_{A \rightarrow L} = -\hat{\mathbf{x}}_{A \rightarrow R}$ , which can be true only when  $\mathbf{x}_A$  is on the perimeter. Therefore, we have the bound  $|(\hat{\mathbf{x}}_{A \rightarrow L} - \hat{\mathbf{x}}_{A \rightarrow R}) \cdot \mathbf{u}_A| < 2\nu$ , which gives

$$\begin{aligned} \frac{\nu}{2} \frac{d}{dt}e^2 &= |e| \text{sgn}(e) ((\hat{\mathbf{x}}_{A \rightarrow L} - \hat{\mathbf{x}}_{A \rightarrow R}) \cdot \mathbf{u}_A - 2\nu \text{sgn}(e)) \\ &< -|e|(-2\nu \text{sgn}(e) + 2\nu) \\ &\leq 0. \end{aligned}$$

Therefore, the error is stabilized around 0, implying that  $J_L^* = J_R^*$ . ■

Since the afferent surface extends from the defender's position, the lemma shows that the intruder can only reach the perimeter by passing through the defender position: i.e., it cannot reach the perimeter without getting captured. Therefore, we extend the definition of capture to the condition  $\mathbf{x}_A \in \Gamma_{\text{aff}}(s_D)$ , and use it as part of the terminal condition. Note that this definition contains the narrow condition for capture:  $\mathbf{x}_A = \gamma(s_D) = \mathbf{x}_D$ .

**Lemma 3** *Let  $\mathcal{R}_D(s_D)$  denote the complement of  $\mathcal{R}_A(s_D)$ . If the initial condition is  $\mathbf{x}_A \in \mathcal{R}_D(s_D)$ , i.e.,  $\mathbf{x}_A \notin \mathcal{R}_A(s_D)$ , then regardless of the intruder strategy, the defender wins the game of kind using  $\omega_D^*$  in (17): i.e., the defender either captures the intruder or prevents it from scoring indefinitely.*

**PROOF.** Suppose the intruder stays outside of the winning region  $\mathcal{R}_A$ . Then, since  $\mathcal{R}_A$  covers the entire perimeter other than a single point  $s_D$  (defender position), the only entry point to the perimeter is now  $s_D$ . However, entering the perimeter from  $s_D$  means capture. Therefore, for the intruder to win the game, it is necessary to enter  $\mathcal{R}_A$ . The question is: can the intruder start outside of  $\mathcal{R}_A$  and enter it?

Crossing the boundary  $\partial \mathcal{R}_A$  and entering  $\mathcal{R}_A$  requires  $V(s_D, \mathbf{x}_A)$  to increase from negative to positive. However, this is impossible when  $\mathbf{x}_A \in \Omega_L(s_D)$  because

$$\dot{V} = \dot{J}_L^* = \frac{1}{\nu} \hat{\mathbf{x}}_{A \rightarrow L} \cdot \mathbf{u}_A - \omega_D^* \leq 0. \quad (19)$$

We similarly have  $\dot{V} \leq 0$  for  $\mathbf{x}_A \in \Omega_R(s_D)$ . Therefore,  $V(s_D, \mathbf{x}_A)$  is non increasing, and so the intruder cannot enter the region  $V > V(t_0)$ , implying that it cannot enter  $\mathcal{R}_A$ . ■

The results of this section is summarized in the following theorem:

**Theorem 1** *The level curve  $V(s_D, \mathbf{x}_A) = 0$  is the barrier of the game of kind.*

The result directly follows from Lemmas 1, 2 and 3.

### 3.3 Optimality of the Strategies

This section discusses how the strategy set  $(\omega_D^*, \mathbf{u}_A^*)$  defined in (17) and (15) forms an equilibrium also in the game of degree for some objective functions. We visit intruder-winning and defender-winning configurations separately.

Suppose the initial configuration is  $\mathbf{x}_A \in \mathcal{R}_A(s_D)$ . Then consider the following objective function:

$$P_1(\omega_D, \mathbf{u}_A) = \min\{s_{D \rightarrow B}(t_F), s_{B \rightarrow D}(t_F)\}, \quad (20)$$

where  $t_F$  is the time the intruder breaches the perimeter at point  $s_B$ . This quantity  $P_1$  describes the *safe distance* at the time of breaching which the intruder maximizes and the defender minimizes. The min operator is used to account for both ccw and cw measure for the distance.

**Theorem 2** *If the initial configuration is  $\mathbf{x}_A \in \mathcal{R}_A(s_D)$ , and if the players use  $P_1$  in (20) as the objective function, then  $\mathbf{u}_A^*$  in (17) and  $\omega_D^*$  in (15) form equilibrium strategies, and the value of the game is  $V(s_D, \mathbf{x}_A)$  in (13):*

$$V = \min_{\omega_D} \max_{\mathbf{u}_A} P_1(\omega_D, \mathbf{u}_A) = \max_{\mathbf{u}_A} \min_{\omega_D} P_1(\omega_D, \mathbf{u}_A) \quad (21)$$

**PROOF.** Suppose  $\mathbf{x}_A \in \Omega_L$  without the loss of generality. Along the terminal surface  $\{[s_D, \mathbf{x}_A] \mid \mathbf{x}_A \in \partial\mathcal{T}\}$ , we have  $\mathbf{x}_A = \gamma(s_B)$  where  $s_B \in \mathcal{S}_L$  from the supposition. We also have  $V = J_L^*(s_D, \mathbf{x}_A) = s_{D \rightarrow B}$  since the term  $\|\gamma(s_L) - \mathbf{x}_A\|$  in (2) is 0. Noting that  $s_{D \rightarrow B} = \min\{s_{D \rightarrow B}, s_{B \rightarrow D}\}$  for  $s_B \in \mathcal{S}_L$ , we have  $P_1 = J_L^*$  along the terminal surface. Therefore, maximizing or minimizing  $P_1$  is equivalent to maximizing or minimizing  $J_L^*(t_F)$  on the terminal surface. Recalling the time derivative in (18), we have

$$1 = \arg \min_{\omega_D} \max_{\mathbf{u}_A} \dot{J}_L^*(\omega_D, \mathbf{u}_A)$$

$$\nu \hat{\mathbf{x}}_{A \rightarrow L} = \arg \max_{\mathbf{u}_A} \min_{\omega_D} \dot{J}_L^*(\omega_D, \mathbf{u}_A)$$

and

$$\min_{\omega_D} \max_{\mathbf{u}_A} \dot{J}_L^*(\omega_D, \mathbf{u}_A) = \dot{J}_L^*(1, \nu \hat{\mathbf{x}}_{A \rightarrow L}) = 0.$$

The above results prove the theorem. ■

**Remark 3** *A similar result is obtained for any objective function that is an increasing function of  $P_1$ . For example, let  $\alpha : [0, L/2) \rightarrow [0, \infty)$  be a strictly increasing function. Then  $P' \triangleq \alpha(P_1)$  is a valid objective function that*

has  $\mathbf{u}_A^*$  in (17) and  $\omega_D^*$  in (15) as the equilibrium strategies. The value of the game is then  $V' = \alpha(V)$ . The proof relies on the fact that  $P_1 = V$  along the terminal surface and  $\dot{V} = 0$  everywhere under the optimal strategies.

**Remark 4** *If the intruder's objective is to quickly reach the perimeter, e.g.,  $P' = -(t_F - t_0)$ , then the optimal intrusion strategy will be different. In this case, the intruder will move straight towards the closest point on the perimeter whenever possible (i.e., guarantees no capture). Otherwise, it will choose the breaching point so that it barely avoids the defender, instead of maximizing the safe distance.*

**Remark 5** *The shortest path towards any  $s_B$  outside of  $\mathcal{S}_d$  consists of a straight line towards the tangent point and the path along the perimeter, which is equivalent to breaching the perimeter at the tangent point. Therefore, it is reasonable for the intruder to choose  $s_B$  from  $\mathcal{S}_d$ .*

In the defender winning scenario, we can consider the following quantity which describes the distance of the intruder from the barrier:

$$d_{\text{bar}} = \min_{\mathbf{x} \in \mathcal{R}_A(s_D)} \|\mathbf{x} - \mathbf{x}_A\|. \quad (22)$$

This quantity can be interpreted as a buffer / margin from the intruder winning configuration. The defender will want to maximize this buffer, whereas the intruder can minimize  $d_{\text{bar}}$  hoping that any ‘‘mistake’’ in defender's behavior will let it penetrate the barrier and enter  $\mathcal{R}_A(s_D)$ .

The terminal payoff function is chosen to be the distance from the barrier when the capture occurs at time  $t_F$ :

$$P_2(\omega_D, \mathbf{u}_A) \triangleq -d_{\text{bar}}(t_F) < 0. \quad (23)$$

Note that capture is defined by  $\mathbf{x}_A \in \Gamma_{\text{aff}}(s_D)$  (see the paragraph before Lemma 3). The defender tries to minimize this function, while the intruder tries to maximize it.

**Theorem 3** *If the initial configuration is  $\mathbf{x}_A \notin \mathcal{R}_A(s_D)$ , and if the players use  $P_2$  in (23) as the objective function, then  $\mathbf{u}_A^*$  in (17) and  $\omega_D^*$  in (15) form equilibrium strategies, and the value of the game is  $V(s_D, \mathbf{x}_A)$  in (13):*

$$V = \min_{\omega_D} \max_{\mathbf{u}_A} P_2(\omega_D, \mathbf{u}_A) = \max_{\mathbf{u}_A} \min_{\omega_D} P_2(\omega_D, \mathbf{u}_A). \quad (24)$$

**PROOF.** Following the proof of Theorem 2, the proof is completed if we can show the following identity:

$$-d_{\text{bar}}(s_D, \mathbf{x}_A) = \begin{cases} \nu J_L^*(s_D, \mathbf{x}_A) & \text{if } \mathbf{x}_A \in \Omega_L(s_D) \\ \nu J_R^*(s_D, \mathbf{x}_A) & \text{otherwise.} \end{cases} \quad (25)$$

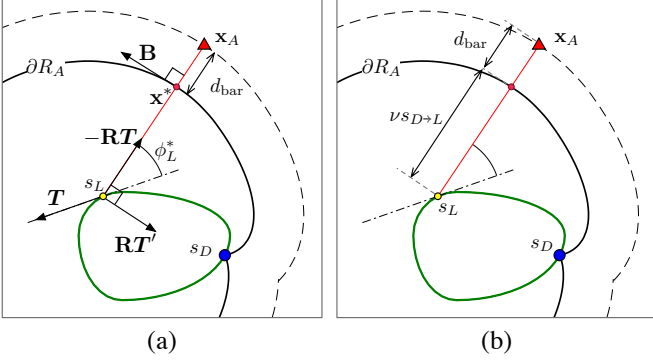


Fig. 7. Proof of the identity  $d_{\text{bar}} = -\nu J_L^*$ .

In the following we prove the case with  $\mathbf{x}_A \in \Omega_L(s_D)$ .

We first show that the point  $\mathbf{x}^* \in \mathcal{R}_A$  closest from  $\mathbf{x}_A$  lies on the straight line from  $\mathbf{x}_A$  to  $\gamma(s_L)$  (see Fig. 7). It suffices to show that  $\mathbf{x}_{A \rightarrow L}$  is perpendicular to the tangent of the barrier  $\partial\mathcal{R}_A$  at  $\mathbf{x}^*$ , denoted by  $\mathbf{B}$ .

We can treat  $s_L$  as a parameter to express a point,  $\mathbf{x}_{\text{bar}}$ , on the left barrier  $\partial\mathcal{R}_A$  as follows:

$$\mathbf{x}_{\text{bar}}(s_L) = \gamma(s_L) - \nu s_{D \rightarrow L} \mathbf{R} \mathbf{T}(s_L),$$

where  $\mathbf{R} \in \mathbb{R}^{2 \times 2}$  denotes the matrix for ccw rotation by  $\phi_L^*$ . The tangent is obtained by

$$\mathbf{B} \triangleq \frac{d\mathbf{x}_{\text{bar}}}{ds_L} = \mathbf{T} - \nu \mathbf{R} \mathbf{T} - \nu s_{D \rightarrow L} \mathbf{R} \mathbf{T}',$$

where  $\mathbf{T}' = \frac{d\mathbf{T}(s_L)}{ds_L}$  denotes the normal vector of  $\gamma$ . The inner product with  $\hat{\mathbf{x}}_{A \rightarrow L}$  gives

$$\begin{aligned} \mathbf{B} \cdot \hat{\mathbf{x}}_{A \rightarrow L} &= \mathbf{T} \cdot \hat{\mathbf{x}}_{A \rightarrow L} - \nu \mathbf{R} \mathbf{T} \cdot \hat{\mathbf{x}}_{A \rightarrow L} - \nu s_{D \rightarrow L} \mathbf{R} \mathbf{T}' \cdot \hat{\mathbf{x}}_{A \rightarrow L} \\ &= \cos(\phi_L^*) - \nu (\hat{\mathbf{x}}_{A \rightarrow L} \cdot \hat{\mathbf{x}}_{A \rightarrow L}) - 0 \\ &= 0, \end{aligned}$$

where from the first to second line we used  $\mathbf{R} \mathbf{T} = \hat{\mathbf{x}}_{A \rightarrow L}$  and  $\mathbf{R} \mathbf{T}' \cdot \hat{\mathbf{x}}_{A \rightarrow L} = -(\mathbf{R} \mathbf{T}' \cdot \mathbf{R} \mathbf{T}) = 0$ .

Now, the distance between  $\mathbf{x}_A$  and  $\mathbf{x}^*$  is

$$d_{\text{bar}} = \|\mathbf{x}_{A \rightarrow L}\| - \nu s_{D \rightarrow L} = -\nu J_L^*.$$

The case with  $\mathbf{x}_A \in \Omega_R$  can be shown similarly. ■

Unlike the intruder strategy, it is easy to see that the defender strategy will stay the same even if the objective is chosen to be the minimum time capture.

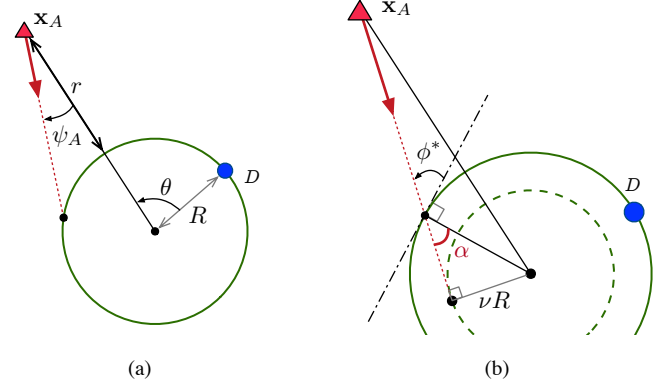


Fig. 8. Circular perimeter case. (a) States  $[r, \theta]$  and the intruder's heading angle  $\psi_A$ . (b) Computation of the approach angle  $\phi^*$ .

### 3.4 Special Cases

We describe two special cases: circular perimeter case, and equal speed case. Since these cases were studied in our previous work [30], we simply state the results and focus on the relation with the results provided in this paper.

When the perimeter is a circle with radius  $R$ , the symmetry allows us to reduce the state space to  $[r, \theta]$ , where  $r$  is the intruder's radial distance from the perimeter, and  $\theta \in [-\pi, \pi]$  is the relative polar angle between the defender and the intruder with respect to the center of the circle.

Whether the intruder is in the left region or the right region is determined by the sign of  $\theta$ :  $\mathbf{x}_A \in \Omega_L(s_D)$  if  $\theta > 0$ , and  $\mathbf{x}_A \in \Omega_R(s_D)$  if  $\theta < 0$ . The singular surfaces correspond to the lines  $\theta = 0$  and  $\theta = \pm\pi$ . The intruder control is parameterized by its speed  $v_A$  and the heading  $\psi_A$  as shown in Fig. 8a.

**Theorem 4 (from [30])** For a circular perimeter, the optimal strategies are

$$\omega_D^* = \text{sgn}(\theta), \text{ and} \quad (26)$$

$$(v_A^*, \psi_A^*) = \left( \nu, \text{sgn}(\theta) \sin^{-1} \left( \frac{\nu R}{R+r} \right) \right), \quad (27)$$

and the value of the game is

$$V(r, \theta; \nu) = |\theta| - F(r) + F(0), \quad (28)$$

where

$$F(r) = \sqrt{\left( \frac{R+r}{\nu R} \right)^2 - 1} - \cos^{-1} \left( \frac{\nu R}{R+r} \right). \quad (29)$$

The sign function accommodates the switching between the left and the right regions.

The intrusion strategy further allows a geometric interpretation: the optimal path of the intruder is to move towards the tangent point of the circle with radius  $\nu R$  (see Fig. 8b) [30]. To verify this result with the strategy given in (15), we compute the approach angle as follows. The angle  $\alpha$  in Fig. 8b is  $\alpha = \sin^{-1}(\frac{\nu R}{R}) = \sin^{-1}(\nu)$ . The approach angle is  $\phi^* = \pi - \frac{\pi}{2} - \alpha = \frac{\pi}{2} - \sin^{-1}(\nu)$ , which reduces to the relation  $\phi^* = \cos^{-1}(\nu)$ . Recalling the results in (4), the circular case matches with our analysis in this paper.

The other special case is when the speed ratio is  $\nu = 1$ . Notice that the objective function now has the form  $J_L^* = s_{D \rightarrow L} - \|\mathbf{x}_{A \rightarrow L}\|$ , in which case the level set  $V = 0$  is generated by the locus of intruder positions where  $\|\mathbf{x}_{A \rightarrow L}\| = s_{D \rightarrow L}$  (and similarly for the right breaching points). In addition, recalling Remark 1, the optimal breaching points are  $s_L = s_{\tan, L}$  and  $s_R = s_{\tan, R}$ . These properties are sufficient to see that the barrier  $\partial \mathcal{R}_A$  is given by a curve called the *involute* — a locus of the tip of a taut string unwound from the geometry. The left and the right part of the barrier corresponds to unwinding the string in ccw and cw directions.

## 4 Two vs. One Game

The next building block is the game played between two defenders ( $D_i, D_j$ ) and one intruder. The states of the system are now  $[s_{D_i}, s_{D_j}, \mathbf{x}_A]$ . We follow the same structure as the previous section and discuss both the game of kind and the game of degree.

### 4.1 Geometries

A naive extension of the two-player game will conclude that the intruder will win if it is in the winning region against both defenders  $D_i$  and  $D_j$ , i.e., if  $\mathbf{x}_A$  is in

$$\mathcal{R}_I \triangleq \{\mathbf{x} \mid V(s_{D_i}, \mathbf{x}) > 0 \text{ and } V(s_{D_j}, \mathbf{x}) > 0\}. \quad (30)$$

The subscript  $I$  is used to reflect the fact that the games against  $D_i$  and  $D_j$  are *independently* considered. However, since the intruder has to avoid both  $D_i$  and  $D_j$  simultaneously, the optimal intrusion strategy and the winning regions are now different.

Observe that now the game space is divided into two parts by  $\Gamma_{\text{aff}}(s_{D_i})$  and  $\Gamma_{\text{aff}}(s_{D_j})$  (see Fig. 9a). We showed in Sec. 3.2 that the intruder cannot win if it reaches the afferent surface, so we include  $\mathbf{x}_A \in \Gamma_{\text{aff}}(s_{D_i}) \cup \Gamma_{\text{aff}}(s_{D_j})$  as part of the terminal condition. Since  $\mathbf{x}_A$  never crosses these surfaces, we can focus our attention on the region that contains the intruder and ignore the other. Without

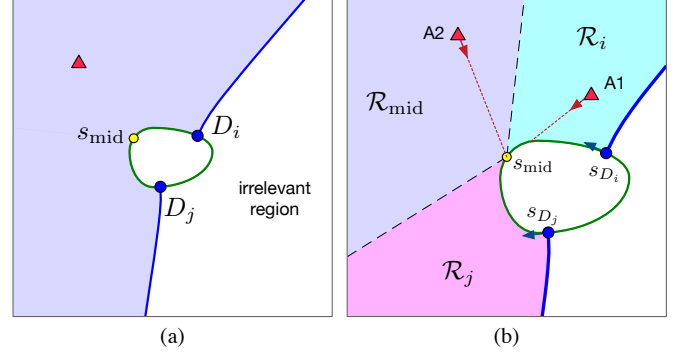


Fig. 9. (a) Game space divided by the two afferent surfaces. (b) Further division into three regions based on the location of the left and right breaching points.

the loss of generality, we define  $D_i$  to be the one on the cw side and  $D_j$  to be the one on ccw side (Fig. 9a).

The opposite point  $s_D^{\text{op}}$  was important in the two-player game because it was the farthest point from the defender. The analogy in the two vs. one game is the midpoint,  $s_{\text{mid}}$ , between the two defenders, which achieves the maximum distance from the nearest defender.

In deriving the intruder strategy, we consider the following quantity:

$$J_{ij} = \min\{s_{D_i \rightarrow B}, s_{B \rightarrow D_j}\} - \frac{1}{\nu} \|\gamma(s_B) - \mathbf{x}_A\|. \quad (31)$$

The interpretation is similar to  $J_L$  and  $J_R$  in Sec. 3. It is the expected safe distance assuming that (i)  $D_i$  moves ccw, (ii)  $D_j$  moves cw, and (iii) the intruder moves on a straight line path towards some breaching point  $s_B$ .

For this function, we can consider three cases depending on where  $s_B$  lies in:

$$J_{ij} = \begin{cases} J_L(s_B; s_{D_i}, \mathbf{x}_A) & \text{if } s_B \in [s_{D_i}, s_{\text{mid}}) \\ J_R(s_B; s_{D_j}, \mathbf{x}_A) & \text{if } s_B \in (s_{\text{mid}}, s_{D_j}] \\ J_{\text{mid}}(s_{D_i}, s_{D_j}, \mathbf{x}_A) & \text{otherwise: } s_B = s_{\text{mid}}, \end{cases} \quad (32)$$

where

$$J_{\text{mid}} \triangleq \frac{1}{2} s_{D_i \rightarrow D_j} - \frac{1}{\nu} \|\gamma(s_{\text{mid}}) - \mathbf{x}_A\|. \quad (33)$$

Such division is possible because only  $D_i$ 's position is active in the calculation of  $J_{ij}$  when the breaching point is in  $[s_{D_i}, s_{\text{mid}})$ , and similarly only  $D_j$ 's position matters when  $s_B \in (s_{\text{mid}}, s_{D_j}]$ .

The game space that contains the intruder can be further

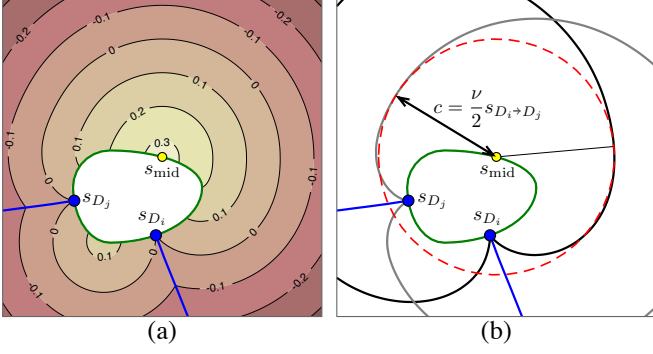


Fig. 10. (a) Level set of  $V_{ij}$ . (b) Geometric construction of the zero level set of  $V_{ij}$ .

divided into three regions (see Fig. 9b):

$$\begin{aligned} \mathcal{R}_i &= \{\mathbf{x}_A \mid s_L \in [s_{D_i}, s_{\text{mid}}]\} \\ \mathcal{R}_j &= \{\mathbf{x}_A \mid s_R \in [s_{\text{mid}}, s_{D_j}]\} \\ \mathcal{R}_{\text{mid}} &= \{\mathbf{x}_A \mid s_L \notin [s_{D_i}, s_{\text{mid}}], s_R \notin [s_{\text{mid}}, s_{D_j}]\}. \end{aligned} \quad (34)$$

In  $\mathcal{R}_i(s_{D_i}, s_{D_j})$  the intruder can choose  $s_L$  to play optimally against  $D_i$  without considering  $D_j$ , because  $s_{D_j}$  will not be active in  $J_{ij}$ . When in  $\mathcal{R}_{\text{mid}}$ , the intruder cannot simply choose one defender to play against because the optimal behavior against  $D_i$  makes  $D_j$  to be the active defender and vice versa. A good compromise in this case is to approach  $s_{\text{mid}}$ .

Now we have a candidate intrusion strategy:

$$\mathbf{u}_A^* = \nu \hat{\mathbf{x}}_{A \rightarrow \text{opt}} \quad (35)$$

where  $\hat{\mathbf{x}}_{A \rightarrow \text{opt}} = \frac{\gamma(s_{\text{opt}}) - \mathbf{x}_A}{\|\gamma(s_{\text{opt}}) - \mathbf{x}_A\|}$ , and the optimal breaching point is defined by

$$s_{\text{opt}}(\mathbf{x}_A, s_{D_i}, s_{D_j}) = \begin{cases} s_L & \text{if } \mathbf{x}_A \in \mathcal{R}_i(s_{D_i}, s_{D_j}) \\ s_R & \text{if } \mathbf{x}_A \in \mathcal{R}_j(s_{D_i}, s_{D_j}) \\ s_{\text{mid}} & \text{otherwise.} \end{cases} \quad (36)$$

The associated value (to be proved in Theorem 6) is given in the following:

$$V_{ij} = \begin{cases} J_L^*(s_{D_i}, \mathbf{x}_A) & \text{if } \mathbf{x}_A \in \mathcal{R}_i(s_{D_i}, s_{D_j}) \\ J_R^*(s_{D_j}, \mathbf{x}_A) & \text{if } \mathbf{x}_A \in \mathcal{R}_j(s_{D_i}, s_{D_j}) \\ J_{\text{mid}}(s_{D_i}, s_{D_j}, \mathbf{x}_A) & \text{otherwise,} \end{cases} \quad (37)$$

where the regions are defined in (34). Fig. 10a shows the level sets of  $V_{ij}(s_{D_i}, s_{D_j}, \mathbf{x}_A)$ . Each level set is a combination of three curves: the two level sets from the one vs. one games and a circle centered at  $s_{\text{mid}}$ . Specifically, the zero level set ( $V_{ij} = 0$ ) is a combination of the two barriers, and a circle with radius  $c = \frac{1}{2}\nu s_{D_i \rightarrow D_j}$  (see Fig. 10b).

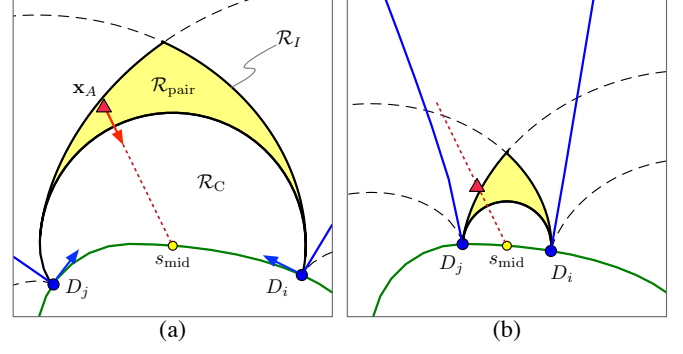


Fig. 11. Paired-defense region. (a) Intruder starts in  $\mathcal{R}_{\text{pair}}$ . Neither  $D_i$  nor  $D_j$  has a guarantee to win from the one vs. one game analysis because  $\mathbf{x}_A \in \mathcal{R}_I$ . (b) Pincer maneuver by the defender pair pushes the intruder out from  $\mathcal{R}_{\text{pair}}$ , while also avoiding it to enter  $\mathcal{R}_C$ . At this time,  $D_j$  can guarantee its victory using one vs. one strategy since  $\mathbf{x}_A \in \mathcal{R}_D(i)$ .

#### 4.2 Winning Regions

Analogous to the two-player game, we define the intruder winning region by

$$\mathcal{R}_C(s_{D_i}, s_{D_j}) \triangleq \{\mathbf{x}_A \mid V_{ij}(s_{D_i}, s_{D_j}, \mathbf{x}_A) > 0\}. \quad (38)$$

The subscript  $C$  is used to highlight the *cooperative* nature of the defense strategy. The following lemma gives a sufficient condition for intruder's victory:

**Lemma 4** *If the initial configuration satisfies  $\mathbf{x}_A(t_0) \in \mathcal{R}_C(s_{D_i}(t_0), s_{D_j}(t_0))$ , then regardless of the defender's strategy, the intruder wins the game of kind using  $\mathbf{u}_A^*$  defined in (35).*

**PROOF.** If the intruder starts in  $\mathcal{R}_i \cap \mathcal{R}_C$ , then it wins against  $D_i$  by approaching  $s_L$  since  $J_L^*(s_{D_i}, \mathbf{x}_A) > 0$ . Although  $s_L$  is suboptimal against  $D_j$ , the intruder still wins because  $s_{L \rightarrow D_j}(t_0) > s_{D_i \rightarrow L}(t_0)$ :  $D_j$  is farther from  $s_L$  than  $D_i$ . With the same argument, intruder wins if it starts in  $\mathcal{R}_j \cap \mathcal{R}_C$ . Finally, if  $\mathbf{x}_A \in \mathcal{R}_{\text{mid}} \cap \mathcal{R}_C$ , then it can reach  $s_{\text{mid}}$  before either of the defenders because  $J_{\text{mid}} > 0$ . ■

Observe that the intruder-winning region  $\mathcal{R}_C$  is smaller than  $\mathcal{R}_I$  derived from the two-player game analysis. The gap is generated by the cooperation between the defenders.

**Definition 4** *The paired-defense region is defined by:*

$$\mathcal{R}_{\text{pair}}(s_{D_i}, s_{D_j}) = \mathcal{R}_I(s_{D_i}, s_{D_j}) - \mathcal{R}_C(s_{D_i}, s_{D_j}). \quad (39)$$

The next lemma shows that  $\mathbf{x}_A \in \mathcal{R}_C$  is also a necessary condition for the intruder to win the game of kind:

**Lemma 5** *If the initial condition is  $\mathbf{x}_A \in \mathcal{R}_{\text{pair}}(s_{D_i}, s_{D_j})$ , and if the defender pair uses a pincer movement  $[\omega_{D_i}, \omega_{D_j}] = [1, -1]$ , then either  $\mathbf{x}_A \in \mathcal{R}_D(s_{D_i})$  or  $\mathbf{x}_A \in \mathcal{R}_D(s_{D_j})$  occurs before the intruder reaches the perimeter: i.e., defender pair wins.*

**PROOF.** Observe that  $\mathcal{R}_{\text{pair}}$  shrinks as the two defender get closer and disappears when the two meet at the midpoint. Hence, the intruder will exit  $\mathcal{R}_{\text{pair}}$  in finite time. There are only three ways to exit  $\mathcal{R}_{\text{pair}}$ : enter  $\mathcal{R}_D(s_{D_i})$ , enter  $\mathcal{R}_D(s_{D_j})$ , or enter  $\mathcal{R}_C(s_{D_i}, s_{D_j})$ . However, the intruder cannot enter  $\mathcal{R}_C$  because its speed  $\nu$  cannot exceed the rate at which the radius of the circle decreases:  $\dot{c} = \frac{1}{2}\nu \frac{d}{dt}(s_{D_i} \rightarrow s_{D_j}) = \frac{1}{2}\nu(-1-1) = -\nu$ . Therefore,  $\mathbf{x}_A$  enters either  $\mathcal{R}_D(s_{D_i})$  or  $\mathcal{R}_D(s_{D_j})$ . ■

Recalling that  $\mathbf{x}_A \in \mathcal{R}_D(s_{D_i}) \cup \mathcal{R}_D(s_{D_j})$  trivially leads to capture based on the solution to the two-player game, the only region that the intruder can guarantee its victory is  $\mathcal{R}_C(s_{D_i}, s_{D_j})$ .

**Theorem 5** *The level curve  $V_{ij}(s_{D_i}, s_{D_j}, \mathbf{x}_A) = 0$  is the barrier of the game of kind.*

The result directly follows from Lemmas 2, 5 and 4.

### 4.3 Optimality of the Strategies

Consider the intruder winning configuration. The payoff function in (20) can be modified to

$$P_1(\omega_{D_i}, \omega_{D_j}, \mathbf{u}_A) = \min\{s_{D_i \rightarrow B}(t_F), s_{B \rightarrow D_j}(t_F)\}, \quad (40)$$

to describe the safe distance at the time of breaching.

**Theorem 6** *If the initial configuration is  $\mathbf{x}_A \in \mathcal{R}_C(s_{D_i}, s_{D_j})$ , and if the players use  $P_1$  in (40) as the objective function, then  $\mathbf{u}_A^*$  in (35), (36) and the pincer maneuver  $[\omega_{D_i}, \omega_{D_j}] = [1, -1]$  form equilibrium strategies, and the value of the game is  $V_{ij}$  in (37).*

**PROOF.** Similar to the proof of Theorem 2, we can see that  $P_2 = V_{ij}$  along the terminal surface. Therefore, the increase (resp. reduction) in  $P_2$  is equivalent to the increase (resp. reduction) in  $V_{ij}(t_F)$ . To prove the optimality, we will show that

$$\dot{V}_{ij}(\omega_D^*, \mathbf{u}_A) \leq \dot{V}_{ij}(\omega_D^*, \mathbf{u}_A^*) = 0 \leq \dot{V}_{ij}(\omega_D, \mathbf{u}_A^*), \quad (41)$$

where  $\omega_D = [\omega_{D_i}, \omega_{D_j}]$ , and  $\omega_D^* = [1, -1]$ . The above inequality indicates that any unilateral change in the strategy will result in a suboptimal performance.

It is straightforward to prove for the case  $\mathbf{x}_A \in \mathcal{R}_i$  using the time derivative  $\dot{J}_L^*$  in the proof of Theorem 2. The case with  $\mathbf{x}_A \in \mathcal{R}_j$  is similarly simple. However, the case  $\mathbf{x}_A \in \mathcal{R}_{\text{mid}}$  has not been considered yet. For example, can the defenders move in the same direction  $\omega_D^* = [1, 1]$  to move  $s_{\text{mid}}$  away from the intruder? We will investigate this using the time derivative  $\dot{V}_{ij} = \dot{J}_{\text{mid}}$ :

$$\begin{aligned} \dot{J}_{\text{mid}} &= \frac{1}{2}(\omega_{D_j} - \omega_{D_i}) - \frac{\hat{\mathbf{x}}_{A \rightarrow \text{mid}}}{\nu} \cdot (\dot{s}_{\text{mid}} \mathbf{T}(s_{\text{mid}}) - \mathbf{u}_A) \\ &= \frac{1}{2}((1 - \beta)\omega_{D_j} - (1 + \beta)\omega_{D_i}) + \frac{1}{\nu} \hat{\mathbf{x}}_{A \rightarrow \text{mid}} \cdot \mathbf{u}_A, \end{aligned}$$

where we used  $\dot{s}_{\text{mid}} = \frac{1}{2}(\omega_{D_j} + \omega_{D_i})$  and defined

$$\beta \triangleq \frac{\hat{\mathbf{x}}_{A \rightarrow \text{mid}} \cdot \mathbf{T}(s_{\text{mid}})}{\nu} = \frac{\cos \phi(s_{\text{mid}})}{\nu}.$$

From the conditions on  $s_L$  and  $s_R$  (see (34)), the approach angle satisfies  $\phi_L^* \leq \phi(s_{\text{mid}}) \leq \phi_R^*$  when  $\mathbf{x}_A \in \mathcal{R}_{\text{mid}}$ . Hence, we have  $|\cos \phi(s_{\text{mid}})| < \nu$ , or equivalently,  $|\beta| < 1$  in  $\mathbf{x}_A \in \mathcal{R}_{\text{mid}}$ . Therefore, both  $1 - \beta$  and  $1 + \beta$  are positive, and we have

$$\begin{aligned} [1, -1] &= \arg \min_{\omega_D} \max_{\mathbf{u}_A} \dot{J}_{\text{mid}}^*(\omega_D, \mathbf{u}_A), \\ \nu \hat{\mathbf{x}}_{A \rightarrow \text{mid}} &= \arg \max_{\mathbf{u}_A} \min_{\omega_D} \dot{J}_{\text{mid}}^*(\omega_D, \mathbf{u}_A), \end{aligned}$$

and  $\min_{\omega_D} \max_{\mathbf{u}_A} \dot{J}_L^*(\omega_D, \mathbf{u}_A) = 0$ , which completes the proof. ■

For the defender winning configuration, we use the same payoff  $P_2$  in (23), with a modification on  $d_{\text{bar}}$  as follows:

$$d_{\text{bar}} = \min_{\mathbf{x} \in \mathcal{R}_C} \|\mathbf{x} - \mathbf{x}_A\|. \quad (42)$$

**Theorem 7** *If the initial configuration is  $\mathbf{x}_A \notin \mathcal{R}_C(s_{D_i}, s_{D_j})$ , and if the players use  $P_2$  in (23) as the objective function, then  $\mathbf{u}_A^*$  in (35) and the pincer maneuver  $[\omega_{D_i}, \omega_{D_j}] = [1, -1]$  form equilibrium strategies, and the value of the game is  $V_{ij}$  in (37).*

**PROOF.** Similar to the proof of Theorem 3, it suffices to show that  $-\nu d_{\text{bar}} = V_{ij}$ , since we already have the result (41). The identity for the case with  $\mathbf{x}_A \in \mathcal{R}_i$  or  $\mathbf{x}_A \in \mathcal{R}_j$  is already proved in Theorem 3. When  $\mathbf{x}_A \in \mathcal{R}_{\text{mid}}$ , it is easy to get the result  $\mathbf{B} \cdot \mathbf{x}_{A \rightarrow \text{mid}} = 0$  recalling that the barrier  $\partial \mathcal{R}_C$  in this portion is a circle centered around  $s_{\text{mid}}$ . ■

The optimal behavior of the defender at  $s_{D_i}$  against an intruder at  $\mathbf{x}_A$  may be different based on the existence of the third player  $s_{D_j}$ . In a two-player game  $D_i$  has to

decide between cw and ccw motion based on the location of  $\mathbf{x}_A$  with respect to the dispersal surface  $\Gamma_{\text{dis}}(s_{D_i})$ , and it is possible that the cw motion is optimal. On the other hand, in a two vs. one game  $D_i$  (defined as the one on cw side) should always move ccw.

**Remark 6 (Computation)** *Importantly, the calculation of the optimal strategies and the value (for both 1 vs. 1 and 2 vs. 1) do not require an explicit computation of the surfaces nor the regions. Both the intruder and the defender need the following computation:*

- Find the breaching points  $s_L(\mathbf{x}_A)$  and  $s_R(\mathbf{x}_A)$
- Determine  $\mathbf{x}_A \in \Omega_L(s_D)$  or not using (13)
- Determine  $D_i$  and  $D_j$  (cw and ccw defender)
- Compute the objective functions  $J_L^*$ ,  $J_R^*$ , and  $J_{\text{mid}}^*$
- Determine the region using (34)

Once the region is known, the strategy and the value are uniquely determined by (36) and (37). A search is performed only in the first step when finding the breaching points, which is also simple recalling the monotonic behavior of the approach angle  $\phi(s)$ .

## 5 Multiplayer Game

This section discusses how the game changes when there are multiple players. We first review the assignment method proposed by Chen et al. [6,5]. We then show the benefit of cooperative defense and introduce an extension of the assignment policy. We also present how the optimal intruder strategy changes in the multi-player game.

### 5.1 Maximum Matching (MM) defense

For a given initial configuration  $\{\mathbf{x}_{A_i}\}_{i=1}^{N_A}$  and  $\{s_{D_j}\}_{j=1}^{N_D}$ , the defender-winning regions can be used to determine a set of intruders that each defender can win against:  $D_j$  can be assigned to  $A_i$  if  $\mathbf{x}_{A_i} \notin \mathcal{R}_A(s_{D_j})$ . Again, the defender wins by either capturing the intruder or delaying its intrusion indefinitely (see Sec. 3.2).

One can generate a bipartite graph with intruders and defenders as two sets of nodes. Edges will be drawn from each defender to all the intruders that it can capture. Matching in graph theory refers to finding a set of edges with no shared nodes. Here, this restriction corresponds to the assumption that  $D_j$  can only play an optimal two-player game against at most one intruder at a time. Maximum-cardinality matching (MM) algorithms (see references in [6]) give such an edge set with maximum cardinality.

The edge set is used to assign at most one unique defender to each intruder. If  $D_j$  is assigned to  $A_i$ , then  $D_j$

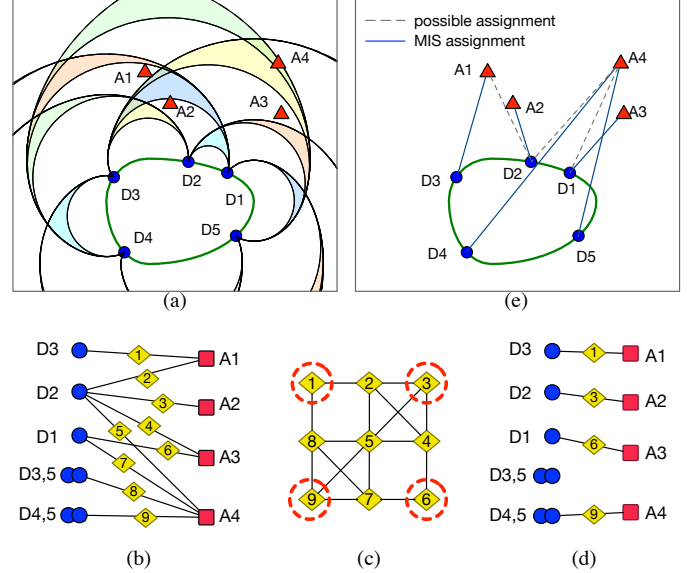


Fig. 12. (a) Example with 5 defenders and 4 intruders. (b) Each node on the left represents a defender or a pair of defenders, and nodes on the right represent intruders. Edges are drawn when the defender or defender pair can win against the intruder. (c) Edges in (b) become nodes in the new graph. A maximum independent set is highlighted in red. (d) An assignment (not necessarily unique) that defends against maximum number of intruders. (e) Assignment described in the original game space.

selects its strategy to be optimal against  $A_i$ . The cardinality of the edge set,  $N_{\text{MM}}^{\text{cap}}$ , tells us that at least  $N_{\text{MM}}^{\text{cap}}$  intruders will be captured. The upper bound on the intruder score is then given by

$$Q_{\text{MM}} = N_A - N_{\text{MM}}^{\text{cap}}. \quad (43)$$

This method assumes that all defenders play independent games and ignores any cooperation with the teammates.

### 5.2 Maximum Independent Set (MIS) defense

Now we allow a defender pair to be assigned to a single intruder. Let  $D_{(i,j)}$  denote a pair  $\{D_i, D_j\}$ . The matching algorithm needs to be modified to avoid conflicts. For example,  $D_i$  and a pair  $D_{(i,j)}$  cannot be treated as independent nodes and be assigned to distinct intruders, because  $D_i$  may not be able to move optimally against two intruders simultaneously. We pose the assignment problem into a maximum independent set (MIS) problem [18] as described in the following:

- 1) Construct a bipartite graph with two sets of nodes  $\mathcal{V}_D = \{D_i\}_{i=1}^{N_D} \cup \{D_{(i,j)}\}_{i \neq j}$  and  $\mathcal{V}_A = \{A_i\}_{i=1}^{N_A}$ . The node set  $\mathcal{V}_D$  now includes all possible defender pairs.
- 2) For each  $D_i$ , draw edges to all intruders,  $A_k$ , such that  $\mathbf{x}_{A_k} \in \mathcal{R}_D(s_{D_i})$ .

- 3) For each pair  $D_{(i,j)}$ , draw edges to all  $A_k$  such that  $\mathbf{x}_{A_k} \in \mathcal{R}_{\text{pair}}(s_{D_i}, s_{D_j})$  (see Fig. 11). Note that we exclude the intruders that are independently capturable by either  $D_i$  or  $D_j$ .

Figure 12a depicts a particular initial condition, and Fig. 12b shows the bipartite graph (nodes with no edges are omitted).

- 4) The edges in the graph are enumerated and become the nodes in the new graph representation (see Fig. 12c).
- 5) Draw an edge between two nodes (in the new graph) whenever they share the same defender or intruder.
- 6) Find MIS, i.e., the largest subset of nodes with no direct connection.

Figures 12d-e illustrate the resultant assignments that give  $N_A^{\text{cap}} = 4$  and  $Q \leq Q_{\text{MIS}} = N_A - N_A^{\text{cap}} = 0$ . Note that the maximum-matching assignment only guarantees  $Q \leq Q_{\text{MM}} = 3$ . For any initial configuration, the MIS formulation gives equal or tighter upper bound because it considers paired defense in addition to all individual defense.

The downside of the above formulation is the fact that MIS cannot be found efficiently [18]. A computationally efficient team policy will appear in a separate publication.

## 6 Simulation Examples

This section demonstrates the theoretical results through numerical examples.

### 6.1 One vs. One Game

We verify the results in Sec. 3 by testing both optimal and suboptimal intrusion strategies. We select the speed ratio to be  $\nu = 0.8$  and start the game in the intruder-winning configuration. Fig. 13a shows the simulation snapshots when the intruder takes the optimal strategy, whereas Fig. 13b and c show the cases when the intruder behaves suboptimally.

By inspecting the right most column, we can compare the performance in terms of two metrics. First, the distance between the defender and the intruder at this time is the *safe distance* considered in Sec. 3.3. We can see that the optimal strategy in Fig. 13a achieves the largest safe distance.

Next, notice the difference in the time the intruder reaches the perimeter. By sacrificing the safe distance, the closest-point strategy in Fig. 13b shows an improved performance in terms of the arrival time. This strategy also has the property of being *open loop* type, since

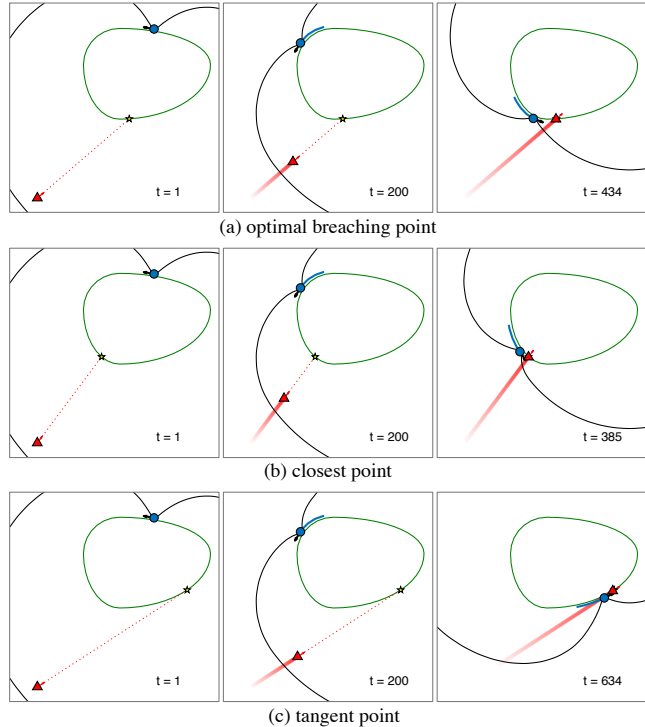


Fig. 13. Simulation snapshots of one vs. one game with  $\nu = 0.8$ . (a) Intruder behavior using the correct speed ratio. (b) Intruder behavior using  $\nu = 0.01$ . (c) Intruder behavior using  $\nu = 1$ .

the closest point on the perimeter is completely independent of the defender's position and/or its behavior. However, note that this strategy does not always guarantee intruder's win even in the intruder winning region. Specifically, when the intruder starts on the barrier curve, only the optimal strategy guarantees its win.

The tangent-point strategy in Fig. 13c shows the opposite effect in the time of arrival. By sacrificing the safe distance, this strategy delays the time the game ends, which may become relevant in a multi-player game where it tries to keep the defender away from other intruders. The result of this example suggests that the optimal strategy will be different if the intruder's objective is to delay the capture as much as possible.

We omit the demonstration of the suboptimal defender strategy since it is already shown clearly with Fig. 6 in Sec. 3.2.

### 6.2 Multiplayer Game

The example provided in Sec. 5 (Fig. 12a) showed a trivial case in which the MIS defense outperforms MM defense, i.e., a case where  $Q_{\text{MM}} \leq Q_{\text{MIS}}$ . Here, we show an example where the two strategies initially have the

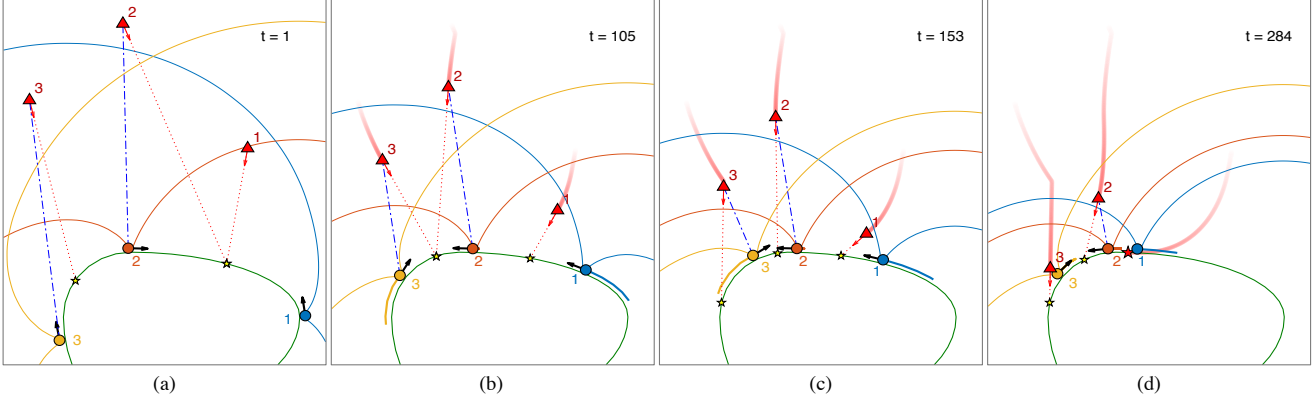


Fig. 14. Simulation snapshots of MM defense.

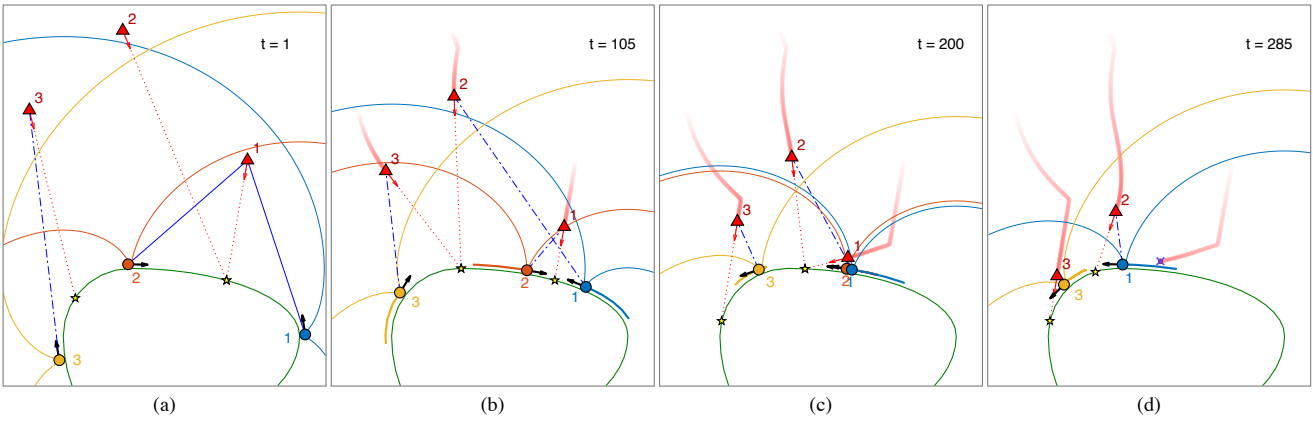


Fig. 15. Simulation snapshots of MIS defense.

same guarantee  $Q_{\text{MM}} = Q_{\text{MIS}}$ , but only MIS actually performs better than the initially provided bound.

Simulation snapshots of a three vs. three scenario are shown in Fig. 14 and 15 for MM defense and MIS defense respectively. The small yellow stars indicate each intruder's breaching point, the dash-dotted lines indicate one vs. one assignments, and the solid blue lines indicate two vs. one assignments.

The intruders are performing independently greedy behavior: i.e., there is no team coordination. Each intruder finds the closest pair of defenders that contains itself in the “relevant region”, defined by the area between the two afferent surfaces (see Fig. 9a). Then the intruder plays the two vs. one game against the pair. For example, in Fig. 14a both  $A_1$  and  $A_2$  are located in the relevant region against the pair  $(D_1, D_2)$ , and therefore move towards the midpoint between the two defenders.

Once the intruder converges on the afferent surface of a defender, the relevant region may start switching frequently. For example, at time  $t = 105$ , the intruder  $A_2$  is already on the afferent surface of defender  $D_2$ . Depending on the side of a small deviation, the relevant pair

for  $A_2$  switches between  $(D_1, D_2)$  and  $(D_2, D_3)$ . Such switching causes the intruder to follow a zigzag path towards defender  $D_2$ . To avoid such degenerate behavior, we add a small bias towards ccw direction when the intruder selects the pair, which is why  $A_2$  selects the pair  $(D_2, D_3)$ . The kink in the path of  $A_3$  (see Fig. 14), is generated due to the switching from the midpoint between  $(D_2, D_3)$  to the one between  $(D_3, D_1)$ .

The MM assignment shown in Fig. 14, has two valid edges giving  $N_A^{\text{cap}} = 2$  and  $Q_{\text{MM}} = N_A - N_A^{\text{cap}} = 1$ . Since this MM assignment does not specify any behavior to unassigned defenders, we also consider a secondary matching between unassigned intruders and defenders. Defender  $D_1$  gets this secondary assignment towards  $A_1$ , which is why  $D_1$  moves ccw. As the  $Q_{\text{MM}}$  from the MM analysis expected,  $A_1$  scores a point (Fig. 14d).

The MIS assignment shown in Fig. 15 also has  $N_A^{\text{cap}} = 2$  at the beginning, only guaranteeing  $Q \leq Q_{\text{MIS}} = 1$ . The pair  $(D_1, D_2)$  initially plays the two vs. one game against  $A_1$ . However, at time  $t = 105$ , the intruder  $A_1$  moves into  $\mathcal{R}_D(D_2)$ , which frees  $D_1$  from the two vs. one game and allows it to perform a one vs. one game against  $A_2$ . At this point, the score upperbound has changed to

$Q_{\text{MIS}} = 0$ , and the defender team guarantees that no intruder scores.

Although the score bound provided by  $Q_{\text{MIS}}$  is tighter than  $Q_{\text{MM}}$  (see Sec. 5), this example highlights that it may still not be the smallest upper bound. Specifically, the MIS analysis could not predict the outcome  $Q = 0$  from the initial configuration. Obtaining a tighter bound is a subject of ongoing work, and it requires the optimal/equilibrium strategies in the team vs. team sense.

We also note that the MIS assignment is non-unique; in fact, it could have selected the same edge set as the MM assignment in this example, because they both have the same cardinality. In other words, the two assignments are equally good in the instantaneous analysis. However, only the assignment shown in Fig. 15 leads to the capture of all intruders. A more sophisticated defender strategy that always makes this “correct” decision is also a part of ongoing work.

## 7 Conclusion

We study a variant of the reach-avoid game with the defenders constrained to move on the perimeter of the target region. The intruders try to score by breaching the perimeter while the defender team tries to minimize the score by intercepting them. The one vs. one game is solved analytically for arbitrary convex shapes, which provides the intruder’s optimal breaching point and the defender’s optimal direction of motion. The derived strategies are at an equilibrium in terms of the safe distance (in the attacker-winning scenario) and the largest margin (in the defender-winning scenario). The two vs. one game is also solved analytically, and it highlights the benefit of cooperation among the defenders. Specifically, two defenders can team up to perform a pincer maneuver to reduce the intruder-winning region. An existing defender assignment method is extended to accommodate the assignment of pairs of defenders. The extension provides a tighter upper bound on the intruder score.

Since the proposed assignment method based on the maximum independent set formulation is computationally inefficient, our ongoing work studies a scalable algorithm without the sacrifice on the performance. We are also studying the optimality (equilibrium) of the team strategies.

## Acknowledgements

We gratefully acknowledge the support of ARL grant ARL DCIST CRA W911NF-17-2-0181.

## References

- [1] Pushkarini Agharkar and Francesco Bullo. Vehicle routing algorithms to intercept escaping targets. *Proc. Amer. Control Conf. (ACC)*, pages 952–957, 2014.
- [2] Efstathios Bakolas and Panagiotis Tsiotras. Relay pursuit of a maneuvering target using dynamic Voronoi diagrams. *Automatica*, 48(9):2213–2220, 2012.
- [3] Tamer Baar and Geert Jan Olsder. *Dynamic Noncooperative Game Theory, 2nd Edition*. Society for Industrial and Applied Mathematics, 2011.
- [4] Shaunak D. Bopardikar, Francesco Bullo, and João P. Hespanha. A cooperative homicidal chauffeur game. *Automatica*, 45(7):1771–1777, 2009.
- [5] Mo Chen, Zhengyuan Zhou, and Claire J. Tomlin. A path defense approach to the multiplayer reach-avoid game. *IEEE Conf. Decision Control (CDC)*, pages 2420–2426, 2014.
- [6] Mo Chen, Zhengyuan Zhou, and Claire J. Tomlin. Multiplayer reach-avoid games via low dimensional solutions and maximum matching. *Proc. Amer. Control Conf. (ACC)*, pages 1444–1449, 2014.
- [7] Timothy H Chung and Geoffrey A Hollinger. Search and pursuit-evasion in mobile robotics. *Auton. Robot.*, 31(4):299–316, 2011.
- [8] Jaime F. Fisac, Mo Chen, Claire J. Tomlin, and S. Shankar Sastry. Reach-avoid problems with time-varying dynamics, targets and constraints. *Proc. 18th Int. Conf. Hybrid Sys. Comp. Control (ACM)*, pages 11–20, 2015.
- [9] Jaime F. Fisac and S. Shankar Sastry. The pursuit-evasion-defense differential game in dynamic constrained environments. *IEEE Conf. Decision Control (CDC)*, pages 4549–4556, 2015.
- [10] Zachariah E. Fuchs, Pramod P. Khargonekar, and Johnny Evers. Cooperative defense within a single-pursuer, two-evader pursuit evasion differential game. *Proceedings of the IEEE Conference on Decision and Control*, pages 3091–3097, 2010.
- [11] Sai Ram Ganti and Yoohwan Kim. Implementation of detection and tracking mechanism for small UAS. *Int. Conf. UAS (ICUAS)*, pages 1254–1260, 2016.
- [12] Eloy Garcia, David W. Casbeer, Khanh Pham, and Meir Pachter. Cooperative aircraft defense from an attacking missile. *J. Guid. Control Dyn.*, 38(8):1510–1520, 2015.
- [13] Haomiao Huang, Jerry Ding, Wei Zhang, and Claire J. Tomlin. A differential game approach to planning in adversarial scenarios: A case study on capture-the-flag. *IEEE Int. Conf. Rob. Autom. (ICRA)*, pages 1451–1456, 2011.
- [14] Haomiao Huang, Wei Zhang, Jerry Ding, Dušan M. Stipanović, and Claire J. Tomlin. Guaranteed decentralized pursuit-evasion in the plane with multiple pursuers. *IEEE Conf. Decision Control (CDC)*, pages 4835–4840, 2011.
- [15] Rufus Isaacs. *Differential games: A mathematical theory with applications to warfare and pursuit, control and optimization*. Courier Corporation, 1999.
- [16] Andrew J. Kerns, Daniel P. Shepard, Jahshan A. Bhatti, and Todd E. Humphreys. Unmanned aircraft capture and control via GPS spoofing. *Journal of Field Robotics*, 31(4):617–636, 2014.
- [17] Tae Hyoung Kim and Toshiharu Sugie. Cooperative control for target-capturing task based on a cyclic pursuit strategy. *Automatica*, 43(8):1426–1431, 2007.

- [18] Eva Kleinberg, Jon and Tardos. *Algorithm design*. Pearson, 2006.
- [19] Li Liang, Fang Deng, Zhihong Peng, Xinxing Li, and Wenzhong Zha. A differential game for cooperative target defense. *Automatica*, 102:58–71, 2019.
- [20] Venkata Ramana Makkapati, Wei Sun, and Panagiotis Tsiotras. Optimal Evading Strategies for Two-Pursuer/One-Evader Problems. *J. Guid. Control Dyn.*, 41(4):851–862, 2018.
- [21] Venkata Ramana Makkapati and Panagiotis Tsiotras. Optimal Evading Strategies and Task Allocation in Multi-player Pursuit/Evasion Problems. *Dynamic Games and Applications*, pages 1–20, 2019.
- [22] Robert Mitchell and Ing Ray Chen. Adaptive intrusion detection of malicious unmanned air vehicles using behavior rule specifications. *IEEE Trans. Syst. Man Cybern.: Syst.*, 44(5):593–604, 2014.
- [23] Dave W. Oyler, Pierre T. Kabamba, and Anouck R. Girard. Pursuit-evasion games in the presence of obstacles. *Automatica*, 65:1–11, 2016.
- [24] Fabio Pasqualetti, Antonio Franchi, and Francesco Bullo. On cooperative patrolling: Optimal trajectories, complexity analysis, and approximation algorithms. *IEEE Trans. Rob.*, 28(3):592–606, 2012.
- [25] Alyssa Pierson, Zijian Wang, and Mac Schwager. Intercepting rogue robots: An algorithm for capturing multiple evaders with multiple pursuers. *IEEE Rob. Autom. Lett.*, 2(2):530–537, 2017.
- [26] Oleg Prokopov and Tal Shima. Linear Quadratic Optimal Cooperative Strategies for Active Aircraft Protection. *J. Guid. Control Dyn.*, 36(3):753–764, 2013.
- [27] Sergey Rubinsky and Shaul Gutman. Three-Player Pursuit and Evasion Conflict. *J. Guid. Control Dyn.*, 37(1):98–110, 2014.
- [28] William Lewis Scott and Naomi Ehrlich Leonard. Optimal evasive strategies for multiple interacting agents with motion constraints. *Automatica*, 94:26–34, aug 2018.
- [29] Jhanani Selvakumar and Efstathios Bakolas. Feedback strategies for a reach-avoid game with a single evader and multiple pursuers. *IEEE Transactions on Cybernetics*, PP:1–12, 2019.
- [30] Daigo Shishika and Vijay Kumar. Local-game decomposition for multiplayer perimeter-defense problem. In *IEEE Conf. Decision Control (CDC)*, pages 2093–2100, 2018.
- [31] Stephen L. Smith, Shaunak D. Bopardikar, and Francesco Bullo. A dynamic boundary guarding problem with translating targets. *Proceedings of the IEEE Conference on Decision and Control*, pages 8543–8548, 2009.
- [32] Zhengyuan Zhou, Wei Zhang, Jerry Ding, Haomiao Huang, Dušan M. Stipanović, and Claire J. Tomlin. Cooperative pursuit with Voronoi partitions. *Automatica*, 72:64–72, 2016.